

Development of a Novel GTAW Process for Joining Ultra-thin Metal Sheets

**Ngo Huu Manh^{1,!}, Van Anh Nguyen^{2,3,*,!}, Han Le Duy⁴, Murata Akihisa², Van Thao
Le^{5,*}, Trinh Quang Ngoc⁴, Bharat Gandham³**

¹ Science-Technology and International Cooperation Department, Sao Do University, Hai Duong, Vietnam

² Research and Development Department, Murata Welding Laboratories, Osaka 5320012, Japan

³ Welding Engineering and Laser Processing Centre, Cranfield University, UK

⁴ Hanoi University of Science and Technology, Hanoi, Vietnam

⁵ Le Quy Don Technical University, Hanoi, Vietnam

* Correspondences:

(VAN) nguyen.van-anh@cranfield.ac.uk

(VTL) vtle@lqdtu.edu.vn

(!) These authors contributed equally to this work and should be regarded as the first joint authors.

Abstract:

The butt weld of ultra-thin sheet raw material coils in production lines is a crucial challenge with traditional welding processes because of the troubles related to the control of heat input, arc stability, application reliability, and investment costs. To overcome such challenges, a novel GTAW process has been developed for joining ultra-thin metal sheets for the first time. The novel welding torch with a novel orifice is the main discovered point of this process. In this paper, the novelties of the developed technology are clarified by comparing it with the conventional GTAW process. The results show that the novel GTAW process features much distinctiveness as compared to the conventional GTAW process: (i) the arc plasma column is more concentrated; (ii) the heat input is considerably reduced, but the temperature at the arc center is greatly increased; (iii) the metal evaporation and the metal vapor amount attached to the tungsten electrode surface are enormously reduced, and (iv) the corrosion of the tungsten electrode tip is vastly reduced. As a result, the novel GTAW process can successfully perform the butt weld of thin/ultra-thin metal sheets (up to 0.03 mm) with high quality and reliability.

Keywords: Novel GTAW process; Novel orifice; Ultra-thin metal sheet; Butt weld; Low heat input.

1. Introduction

Generally, sheet metals are presented in all aspects of modern life. Among sheet metals, thin and ultra-thin sheets are an indispensable part of fabricating high-tech products such as smartphones [1], electronic devices [2], automobiles [3], aerospace [4], and medical equipment [5]. Inside each product, the sheet metal is utilized for small components and miniature parts, such as rotors/stators in the motors, leading frames of integrated circuit (IC) memory chips in smartphones, fine plates in radiators and heat exchangers, envelops in lithium batteries, and connectors in electronic devices [6]. Batch or mass production lines make these products with input materials in thin sheet coils, which need to be exchanged after running out. During the exchange period, the production lines must be stopped and discontinuous (about 60 minutes). Moreover, several dozen meters (about 30 meters) at the end of the material coil and the starting part of the new material coil must be removed to avoid defective products [7]. On the other hand, the length of the raw material sheet in each coil is an average of 1000 meters. From this analysis, it can be considered that more than three percent of the unusable proportion of raw material is in each exchange time. This leads to a significant waste of time and materials. The processing of raw material waste from production lines is expensive and causes environmental pollution (e.g., carbon dioxide emissions) [8]. In order to overcome this issue and make “non-stop” production lines, the butt joint of raw material coils during the operating period becomes an excellent solution. However, due to thin metal sheets that are significantly sensitive to the change of heat inputs, the welding of thin sheets faces many challenges, for example, thermal deformation, burn-through phenomenon, lack of fusion, and unstable weld beads. Any slight change in welding parameters can cause overheating and insufficient heat input, leading to serious defects.

Many investigations have been performed to clarify the influence of welding parameters on the joint formation and mechanical properties and improve the quality of the welded joints of thin and ultra-thin sheets. For instance, Chaudhary et al. [9] applied a pulsed microplasma arc process (micro-PAW) to butt weld thin 316L stainless steel sheets with a thickness of 0.5 mm using a wire of 0.374 mm in diameter. The influences of pulse-on-time and pulse-off-

time factors, torch traveling speed, and peak current on the weld joint strengths were investigated. It was found that the set of parameters, including a duty cycle of 50%, a pulse frequency of 10 Hz, a peak current of 3.5 A, and a torch traveling speed of 250 mm/min, resulted in the maximum joint strength of 553 MPa. The fusion region revealed a minor dissimilarity in microhardness compared to the heat-affected zone. However, a lot of bending and distortion troubles occurred from experimental results. Furthermore, the height of excessive convex at the weldment was double compared to base metal thickness. Tseng et al. [10] also considered the influence of welding parameters (i.e., traveling speed, arc current, arc length, clamping distance, and shielding gas) on the edge joint quality and morphology of 0.1 mm thin stainless steels bellows produced by using the micro-PAW process. The findings demonstrated that the voltage augmented when the additional hydrogen quantity in the argon gas increased. Moreover, the adequate edge butt welds could be produced with a 0.35-mm clamping distance, and the edge welding penetration was about 60% of the thickness. To detect and control in real-time the lack-of-fusion (LoF) defects during the welding of 0.15-mm-thick sheets by the micro-PAW process, Hong et al. [11] developed a monitoring framework using micro-vision sensors, SNNF (symmetric nearest neighbor filter) algorithm and Otsu method. They indicated that the abrupt change in the centroid position of the welding pool along the welding length has a high correlation with LoF, and this parameter could be used to detect the lack of fusion defects in real time. Long et al. [12] utilized the numerical simulation for the butt weld of thin plates with 3 mm in thickness by the metal-inert-gas (MIG) welding process to predict the temperature variation, the fusion and heat-affected zones, the angular distortion, the longitudinal and transverse shrinkage, and residual stresses. They demonstrated that the welding speed and thickness were two factors that significantly influenced residual stress and distortion. Ismail et al. [13] investigated overlap joints between 20 and 50 mm stainless steel sheets using the fiber-laser-welding process. The results showed that the depth and width of weld beads augmented with the welding speed. The use of shielding gas allowed for obtaining uniform beads. Combining high-speed laser scanning and microbeam spot enabled suitable overlap welds of ultra-thin sheets. In another report, Hailat et al. [14]

efforted to butt weld two dissimilar materials – i.e., 0.49-mm-thick Al3003 aluminum and 0.54-mm-thick Cu11000 copper sheets laser micro-welding process. The results pointed out that incorporating Tin-alloy-foil filler between two welded metals could improve the strengths and elongation of joints. The filler incorporation also influenced the solubility of both metals.

Recently, some researchers have investigated and applied the friction stir welding (FSW) process to the butt joint of thin sheets [15]. For instance, Scialpi et al. [16] investigated the mechanical behaviors of joining two aluminum alloys (i.e., 2024-T3 and 6082-T6) sheets with a thickness of 0.8 mm by FSW. The authors stated that the joints revealed good mechanical and fatigue characteristics. Huang et al. [17] used the micro-FSW process to weld ultra-thin sheets Al-6061 sheets. They examined the influence of plunging profile and rotation speed on the surface appearance, microstructure, microhardness, and tensile strength. The optimal plunge depth for 0.5-mm-thick Al6061 aluminum sheets was 0.05 mm. Higher or lower plunging depths than 0.05 mm caused weld defects – e.g., unfilled grooves, thickness reduction, and more powerful flashes. Meanwhile, the increase in rotation velocity could improve the surface characteristics. Yamamoto et al. [18] compared the joining of ultra-high-purity aluminum 0.8-mm-thick sheets by the GTAW and FSW processes. The results showed that the fractures of tensile samples for FSW joints took place in the base metal, whereas the GTAW welded joints were ruptured near the fusion line. Mao et al. [19] focused on the butt welds of 1.0-mm-thick 6061-T6-aluminum alloy and T2-pure-copper ultra-thin sheets produced by micro FSW using different traveling speeds. They showed that the Al-Cu interface featured a good metallurgy bonding because of the Al_2Cu / $AlCu$ / Al_4Cu_9 compound formation. Recently, Moghanni et al. [20] investigated the influence of process parameters in the pinless FSW on microstructural and mechanical characteristics of 1.2-mm-thick Al-0.5Co-Cr-Fe-Ni high-entropy alloy sheets. The authors observed that the heating index played a significant role in the microstructures and mechanical properties of the jointed samples.

Various welding and joining techniques for thin and ultra-thin sheets have been utilized to weld overlap and edge joints. However, no publications about the butt joint of ultra-thin sheets in mentioned manufacturing lines. This is because the troubles related to product quality, reliability, and investment costs are still the main barrier for various applications. In particular, the butt weld of the raw materials used in production lines requires high quality and reliability [21]. The laser welding process is a high-cost and complex welding system. It also requests a very restricted operation safety. Meanwhile, the products produced by the GTAW or PAW process are high tolerance and low reliability. The FSW process also features a high investment cost with a complex equipment system, and the sheet thickness applicable with this process generally ranges from 0.5 to 1 mm [15]. Therefore, their applications in industry to fabricate thin/ultra-thin components are still very limited and not efficient. The production lines using thin/ultra-thin sheets also need breakthrough solutions to avoid stopping time, reduce raw material waste, and improve sustainable production and a clean manufacturing environment. To solve these troubles, a novel GTAW solution is developed in this investigation. The experiments related to the arc plasma phenomena, tungsten electrode wear and weld bead appearance were performed to demonstrate the performance of the novel GTAW process.

2. The novel GTAW process for joining ultra-thin metal sheets

In this investigation, a novel GTAW process for the butt weld without wire feeders has been developed to connect the raw material coils to cut waste time and reduce material waste in mass and batch production lines. The diagram for this production line is shown in Figure 1. In this case, the ultra-thin steel sheets with a thickness of 0.03 to 1.0 mm are used as raw materials. Firstly, the raw material coils are delivered to the workplace. The coil is then pushed and adapted to the manufacturing line. Subsequently, the stamping process is started. When the raw material coil is run out, a new coil is prepared to butt weld with the previous

coil by the novel GTAW process. This process significantly improves the manufacturing lines' productivity, efficiency, and reliability.

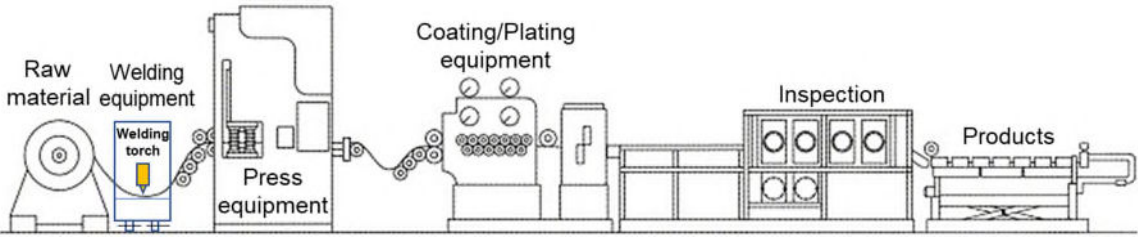


Figure 1. The manufacturing line diagram for ultra-thin sheet metals using a novel GTAW process.

Figure 2 presents the schematic illustration of the novel GTAW equipment and the novel torch. The novel GTAW system includes an adaptive signal box, a CCD camera to observe the molten pool during welding, a control box, a main powder driver box, a push and pull raw material apparatus, and a novel GTAW torch. Figure 3 reveals the schema of the novel torch and the novel orifice. Moreover, the shielding gas is supplied into a back shielding gas box to protect the molten pool and the weldment on the backside. The clamps fix the running out of the raw material coil and the new one. The arc length is automatically controlled to maintain a high accuracy under a circuit board and control program.

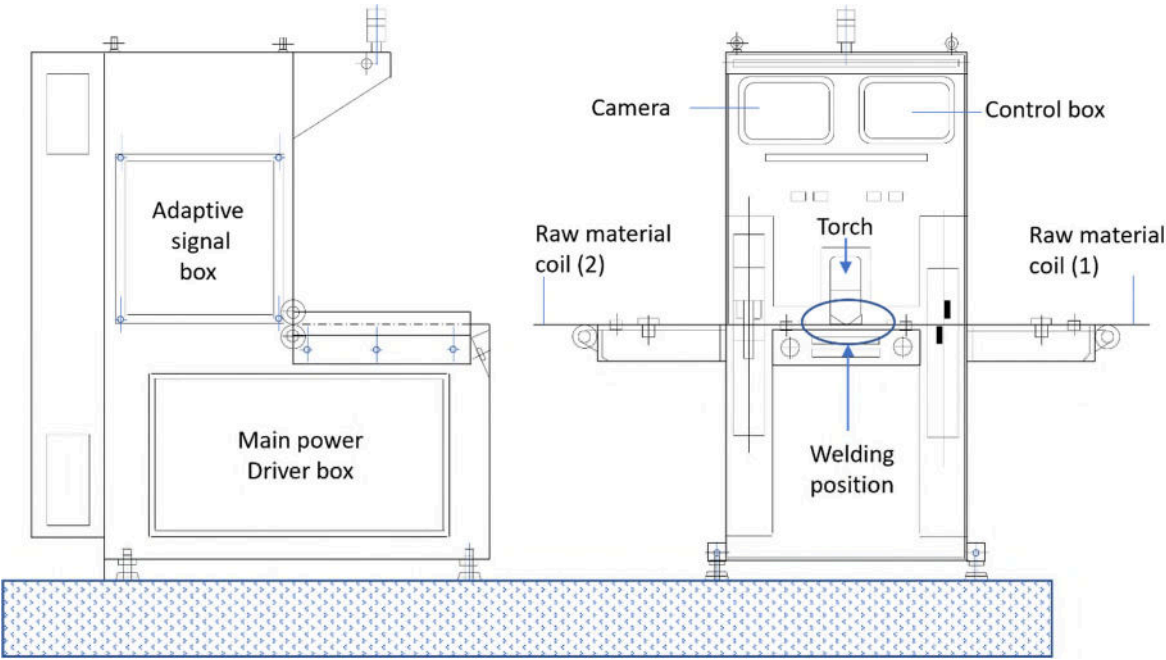
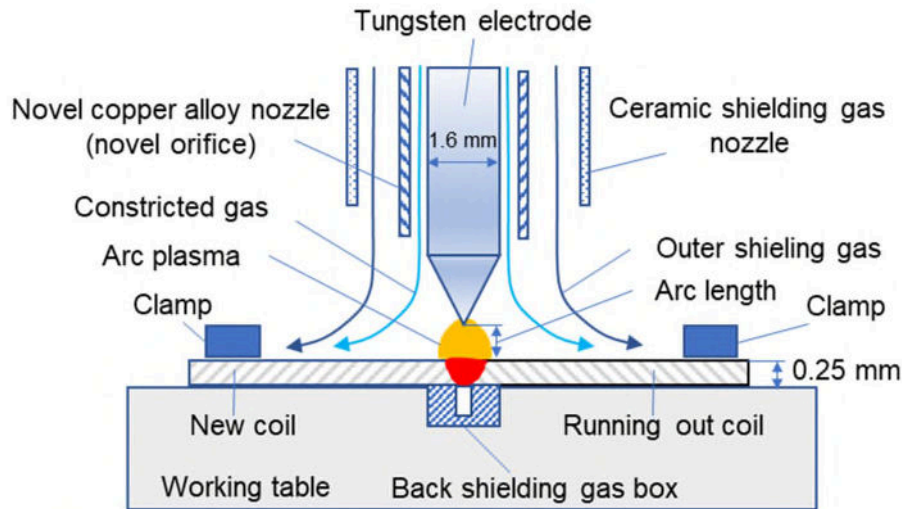
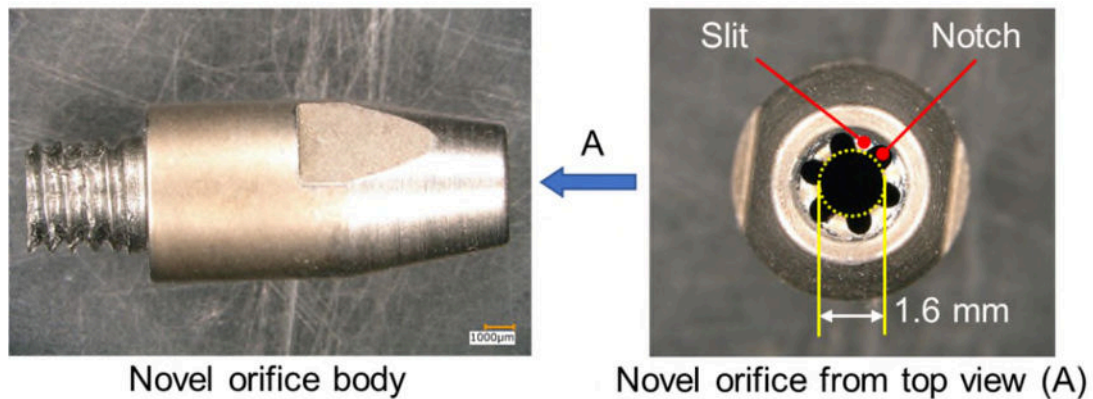


Figure 2. The schematic illustration of the novel GTAW welding system.



(a) novel GTAW torch schematic



(b) novel orifice image

Figure 3. A schematic illustration of the novel GTAW torch and the novel orifice.

The copper-alloy nozzle (novel orifice) is developed and assembled to the torch body in this technology, as shown in Figure 3b. This orifice is reached out of the ceramic shielding gas nozzle (see Figure 3a). The six long slits inside the orifice are contacted with the tungsten electrode to orient the electrode position and control the heat input balance. The tungsten electrode can move alongside (up and down) the orifice, but it is impossible to oscillate horizontally. As a result, the relative position between the tip of the tungsten electrode and the butt joint position can be controlled with high precision.

Among the slits, there are six long notches (Figure 3b on the right). A large amount of the gas flowing from the torch is pushed down along the notches. In addition, a ceramic shielding gas nozzle with a large diameter is utilized to control and orient the shielding gas flow. This ceramic nozzle is similar to the shielding gas nozzle in a conventional GTAW

process. Therefore, the shielding gas consists of constricted gas and outer gas. The novel orifice controls the constricted gas, and the conventional nozzle controls the outer gas. Between these gases, the outer gas has a similar task to the shielding gas flow in the case of the conventional GTAW process. Meanwhile, the constricted gas mainly improves welding efficiency and arc plasma stability.

3. Experimental method

3.1 Welding conditions and equipment.

To demonstrate the performance of the novel GTAW process, two following case studies were considered, including the butt weld of cold-rolled SPCD steel sheets with a thickness of 0.25 mm and a width of 400 mm, and the butt weld of SUS 304 stainless steel sheets of 0.03 mm x 100 mm in thickness and width. The raw materials are contacted together without gaps, and no additional wire is applied in this case. For cutting 0.03 mm plates, a cutting system with very high accuracy is necessary. It requests no the swarf on the cutting kerf. After that, a particular assembled block with the support of a microscope and technical plates to ensure no gap, no overlap, and no miss-match is performed. After that, the microscope head will check the gap, overlap, and mismatch between substrates. The technical plates will be utilized to avoid overlap during the set-up process of substrates. The novel GTAW process was performed on the MWL-400 welding machine of Murata welding laboratories, Co. Ltd, with the novel GTAW torch. The main welding parameters are given in Table 1.

Table 1. Main welding parameters in the novel GTAW process.

Welding parameters	Value/Specifics	
	Case study 1	Case study 2
Base metal	Cold rolled SPCD steel sheets with a thickness of 0.25 mm	SUS 304 stainless steel sheets with a thickness of 0.03 mm
Peak current	30 A	10 A
Bead current	9 A	4 A

Current frequency	120 Hz	120 Hz
Welding speed	2500 mm/min	2500 mm/min
Outer shielding gas and flow rate	Ar, 5 L/min	Ar, 3.0 L/min
Constricted gas and flow rate	Ar, 2.5 L/min	Ar, 1.5 L/min
Back shielding gas	Ar, 2.5 L/min	Ar, 2.5 L/min
Welding current frequency	120 Hz	120 Hz
Arc length	0.25 mm	0.05 mm
Tungsten electrode (diameter)	1.6 mm	1.6 mm
Tip angle of the electrode (whole angle)	60 ⁰	60 ⁰

After the butt weld, the shape and dimensions of the weldment were observed by an optical microscope (VHX-D500, Keyence, Japan). Additionally, the shape and dimensions of the weld bead produced with the novel torch in the first case study – i.e., the butt weld of the cold-rolled SPCD steel sheets with a thickness of 0.25 mm were compared to those of the weld bead achieved by the conventional GTAW torch with the same conditions.

3.2. Temperature distribution and arc phenomena observation

In order to visualize the arc phenomena, the arc length was set up at 1 mm. A high-speed video camera (NAC MEMRECAM GX-1) with a frame rate of 1000 fps was utilized. A cooling water-copper-based anode was used. The arc plasma was captured 10 seconds after starting the arc. Meanwhile, the arc plasma temperature distribution was measured by the spectroscopy technique. The optical system is composed of a spectrometer (Acton SP-2300), a camera lens (Nikon ED AF NIKKOR 70-300 mm), and a high-speed camera (NAC

MEMRECAM GX-1), as illustrated in Figure 4. The ArI-line spectrum of 696.5 nm was used to take photographs. The camera frame rate was set at 1000 fps.

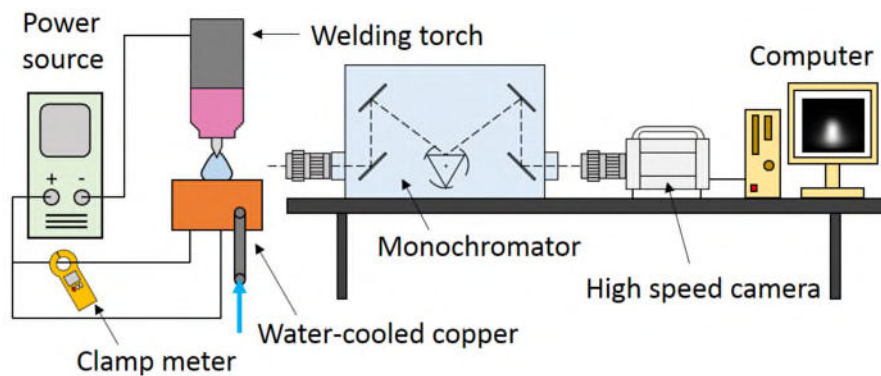


Figure 4. Experimental setup with the spectroscopy technique.

3.3. Tungsten electrode wear observation

To observe the tungsten electrode corrosion phenomena, two tungsten electrodes are prepared and captured before welding by the optical microscope (VHX-D500, Keyence, Japan). They were then installed on the torches (i.e., the novel torch and the conventional GTAW torch). Afterward, the butt welds were done during 60 s with the conventional GTAW torch and the novel GTAW torch, individually with the same welding parameters, as mentioned in Table 1. 60 s is the time from starting until stopping the arc. This duration was controlled and calculated as a part of the controlled program of the developed system. Finally, the electrodes were removed from the torches, and the optical microscope captured the electrode tips (VHX-D500, Keyence, Japan).

4. Experimental results

4.1. Cross-section and weld bead profile

In this paper, five times of welding coils were repeated. And then, the coils were trialed in production lines to verify the welded quality and reliability. The results confirmed that all coils passed through the real working conditions. A typical example of the cross-section and the bead profile is presented in this paper.

The cross-sections of weld beads produced by the novel GTAW torch and the conventional GTAW torch in the first case study were captured in Figure 5. It is revealed that there is a clear difference between the results achieved by the novel torch and the conventional GTAW torch. As compared to the conventional GTAW torch, the novel torch allows producing the weld bead with a narrower bead width on the top side (0.61 mm vs. 0.81 mm) and a more expansive bottom side (0.41 mm vs. 0.31 mm).

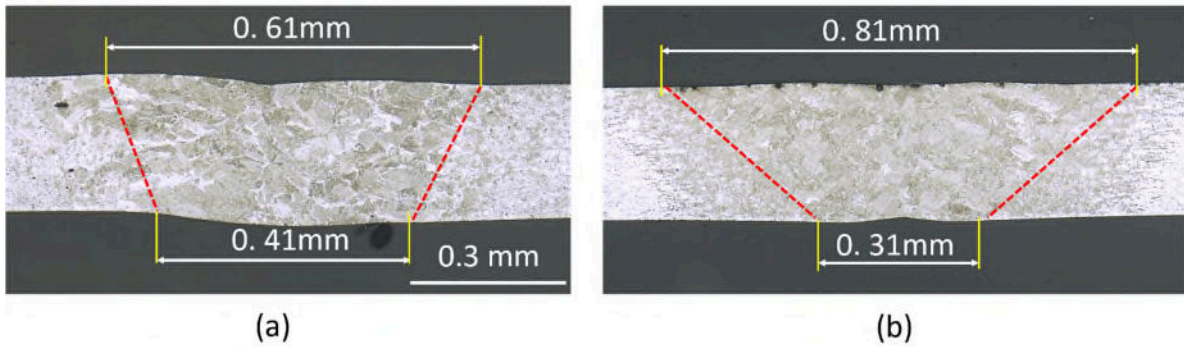


Figure 5. Welding samples of cold-rolled SPCD steel with a thickness of 0.25 mm were produced by (a) the novel GTAW torch and (b) the conventional GTAW torch.

Because the conventional GTAW process is impossible to obtain good quality in the case of super ultra-thin sheets (0.03 mm), in the second case study, only the images of the weld bead profile produced by the novel GTAW process were observed, as presented in Figure 6. It is confirmed that no macro welding defects were observed. The bead width is very stable. The top bead width is about 0.34 mm, and the bottom surface bead width is about 0.26 mm.

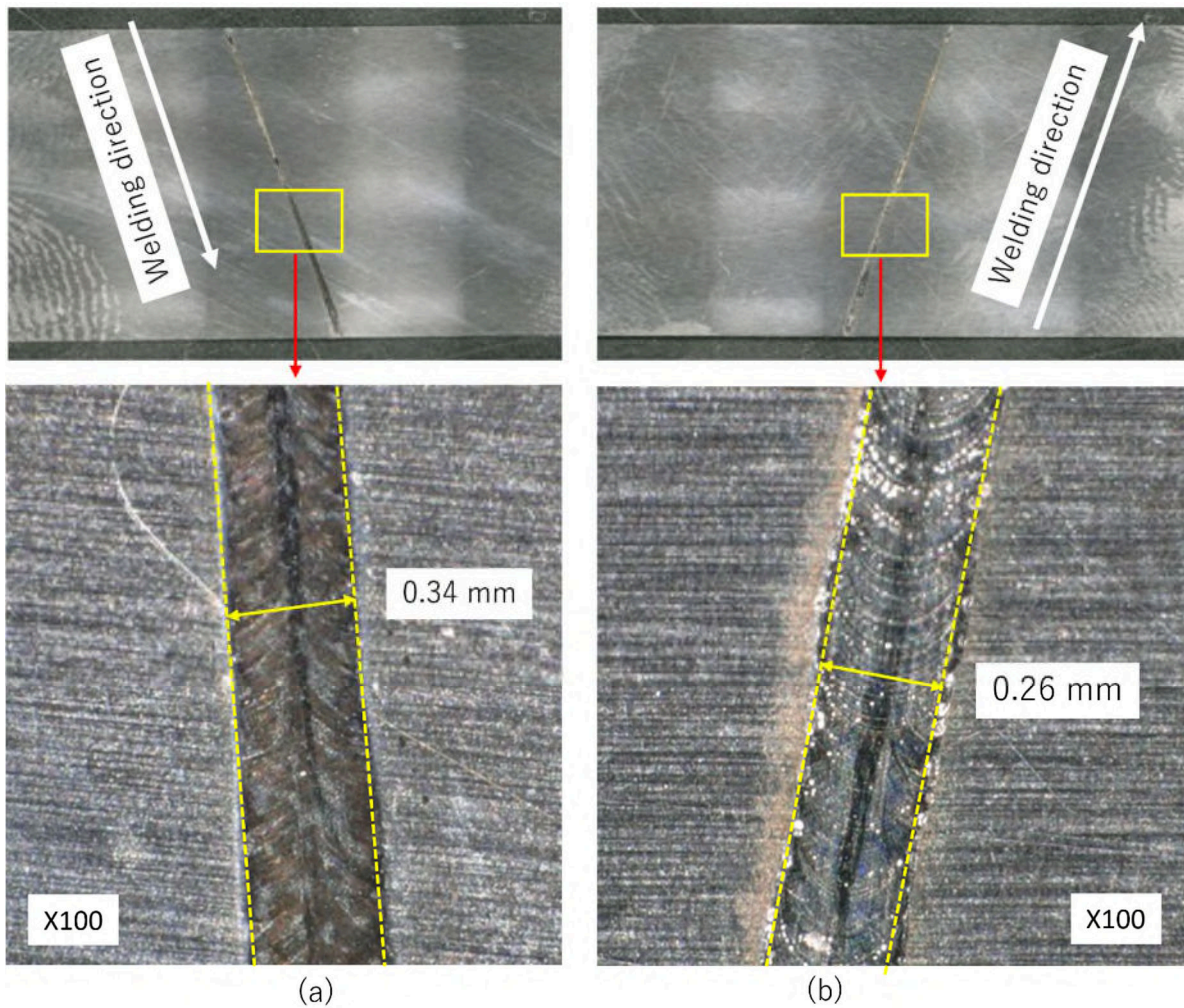


Figure 6. Bead profile of 0.03-mm-thickness SUS stainless steel: (a) top surface and (b) bottom surface.

4.2. Arc plasma and temperature distribution

Figure 7 displays an arc plasma column in the novel GTAW torch and the conventional GTAW torch, where the welding current was set by 30 A. The results indicated that the plasma column is straighter and more constricted in the case of the novel GTAW torch (Figure 7a). The arc plasma column generated by the novel torch is similar to that in the PAW process. The tungsten electrode body is darker, especially within the arc center until the orifice. Meanwhile, the plasma column is wider in the case of a conventional GTAW torch. The tungsten electrode is hotter, with the high-temperature region expanded from the electrode tip until the conventional shielding gas nozzle (Figure 7b).

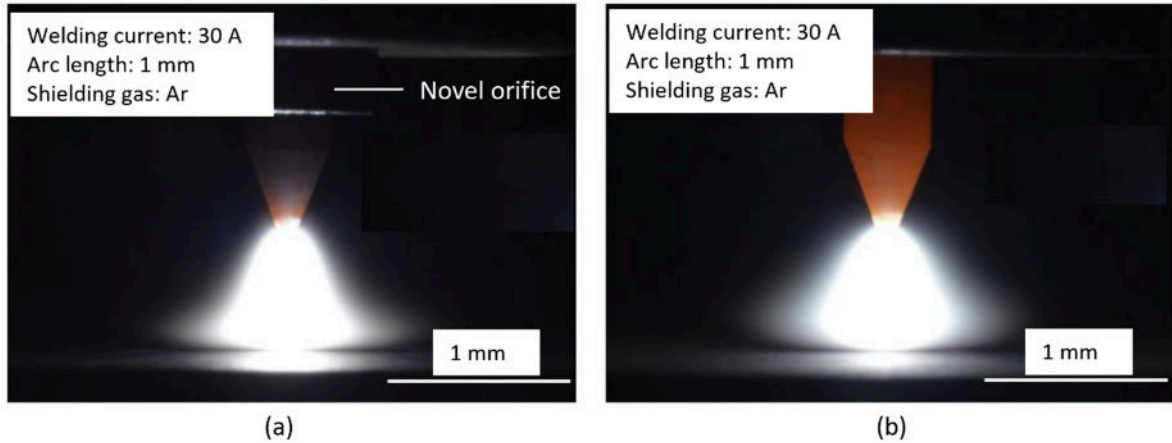


Figure 7. The arc plasma phenomena observation: (a) the novel GTAW torch and (b) the conventional GTAW torch.

Figure 8 portrays the arc plasma temperature distribution in the case the welding current was set by 30 A. There is a distinction between the results achieved by the conventional GTAW torch and the novel torch. The temperature at the center of the arc in the case of the novel GTAW torch (Figure 8a) is much higher than that in the conventional GTAW torch (Figure 8b). In the case of the novel torch, the high-temperature zone is extended alongside the arc column from the tungsten electrode until the copper anode. Meanwhile, the temperature at the arc center in the case of conventional GTAW is much lower and is not alongside the axial.

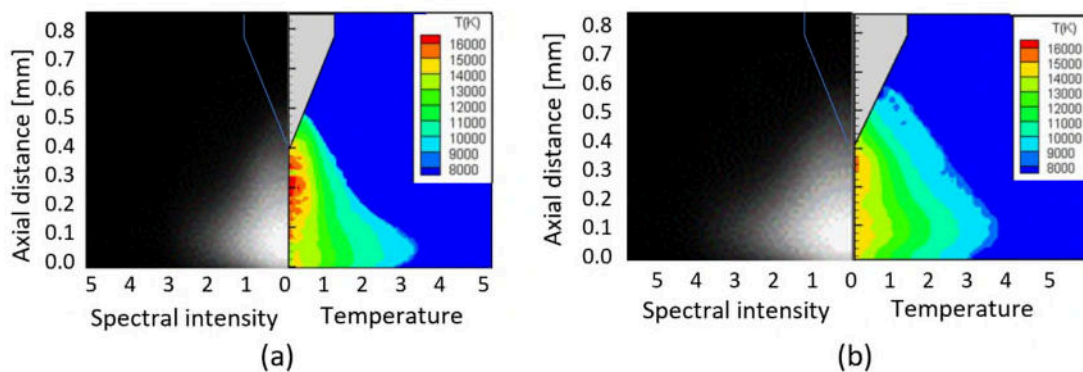


Figure 8. The plasma arc temperature distribution: (a) the novel GTAW torch and (b) the conventional GTAW torch.

4.3. Tungsten electrode wear

Figure 9 reveals the tungsten electrode situation at three periods: before welding, after welding 60 s with the novel torch, and after welding 60 s with a conventional GTAW torch in the first case study. The tip of the electrode before welding was selected as the original point. After welding, the tip of the electrode was burned (corroded), and the distance from the original point was measured and calculated by the optical microscope.

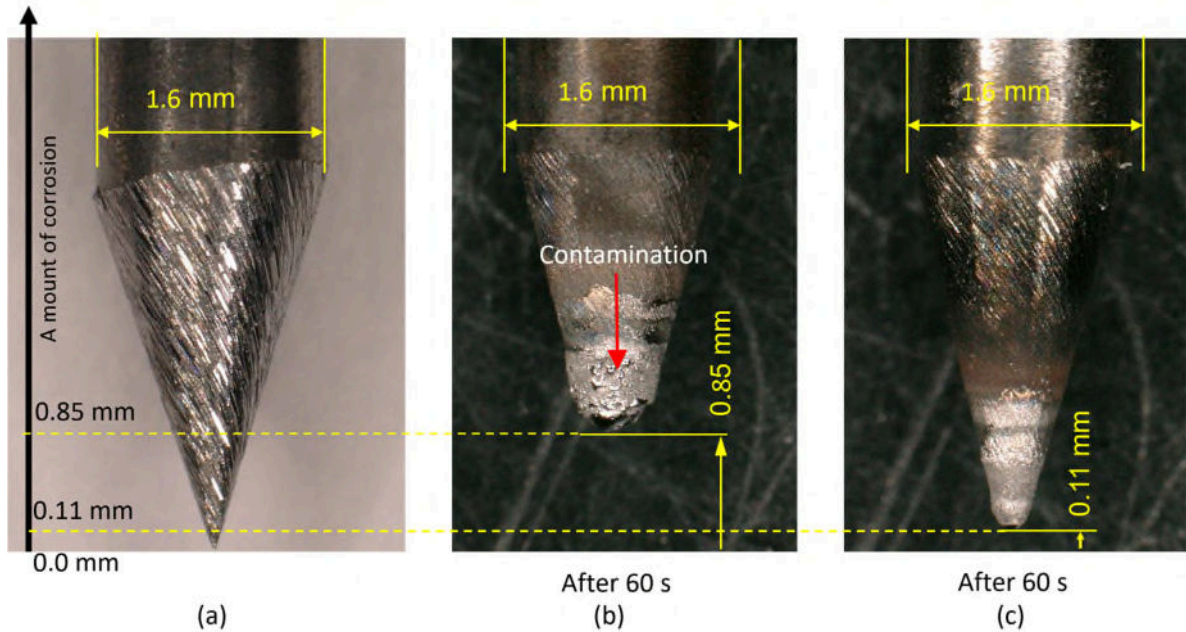


Figure 9. The tungsten electrode situation: (a) before welding, (b) after continuous welding 60 s with the conventional GTAW torch and (c) after continuous welding 60 s with the novel GTAW torch.

It can be clearly seen that, in the case of the conventional GTAW torch, the tungsten electrode is corroded much higher than in the novel torch. The tungsten electrode of the conventional GTAW torch was burned about 0.85 mm (Figure 9b), while that was only about 0.11 mm in the novel GTAW torch (Figure 9c). Much metal from the molten pool is attached to the tungsten electrode tip in the conventional GTAW torch (Figure 9b), resulting in significant contamination on the tungsten electrode surface. On the other hand, the surface of the tungsten electrode in the novel GTAW torch was cleaner than the conventional torch, leading to little contamination on the surface of the tungsten electrode. This means that a small amount of the metal vapor from the molten pool was attached to the tungsten electrode

in the case of the novel torch. In contrast, a large amount of metal vapor from the molten pool was enclosed to the tungsten electrode surface in the case of the conventional GTAW torch.

5. Discussion

The novel welding process has the operating principle (arc discharge mechanism) based on the GTAW process, meaning that the arc is discharged between the positive electrode (i.e., the base metal) and the negative electrode (i.e., the torch/the novel orifice). There is no pilot arc in this novel technology. However, the arc plasma column is with the bell formula and is constricted closely to the arc plasma column in the PAW process. The main advantage points of this novel process are detailed as follows.

5.1 Arc plasma phenomena, melt pool stability, and heat input reduction

In the novel GTAW process, the gas flowing by the novel orifice plays a substantial role in improving priority characteristics, welded stability, and joint quality compared to the conventional GTAW process. Its gas pressure is enormously increased through extreme narrow gaps (notches) between the tungsten electrode and the novel orifice. In this case, the arc column as a bell formula is strongly constricted, as shown in Figure 8a. As a result, the temperature at the center area of the arc column has vastly increased, especially along the centerline. However, in the radial direction, the arc temperature is decreased sharply, similar to that in the conventional GTAW process. On the other hand, the current is controlled in a pulse formula with a frequency of 120 Hz. It means that the current is alternated continuously from peak current to bead current in each cycle of welding current. In combination with the constricted gas flow cooling the melt pool, it can reduce the heat input to ensure a suitable condition to weld ultra-thin sheets efficiently.

If the thickness of base metal is reduced, another essential factor that needs to be controlled carefully is the gas flow rate. For example, in the case of 0.25 mm plates, the constricted gas and the shielding gas were 2.5 l/min and 5.0 l/min, respectively. However, in the case of 0.03 mm, they were 1.5 l/min and 3.0 l/min, respectively. This is related to the melt

pool stability during welding. In the case of the ultra-thin sheet, the melt pool is a very narrow and thin layer. It is susceptible to changing input parameters such as the gas flow rate, especially the constricted gas. This melt pool is blown away easily to cause the cutting or burn-through phenomenon. To control this phenomenon, the reduction of the gas flow rate is studied carefully. Based on this investigation, the suitable gas flow rate was selected with higher (2.5 l/min) in the case of 0.25 mm and lower (1.5 l/min) in the case of 0.03 mm to control the melt pool stability in this paper.

These results verify that, in the case of the novel process, the heat input density increases, but the heat input decreases compared to the conventional GTAW process. Furthermore, a recent simulation study about plasma flow shows that the plasma flow velocity is much different in both cases, novel torch and conventional torch [22]. In the case of the novel torch, the plasma flow velocity is much increased, especially around the center and along the molten metal pool surface. The maximal velocity in the case of the novel torch is two times higher than that in the case of the conventional GTAW torch. In other words, the plasma flow with high speed and high arc pressure is formed by impinging on the base metal surface under the efficiency of the novel orifice to create a very stable and narrow shape for the arc column. Moreover, using a novel orifice accelerates the plasma jet through a high-speed constricted gas flow. Therefore, the thermal pinch effect on the arc plasma, the energy density of the arc plasma, and the electron discharge capacity are significantly improved compared to the conventional GTAW torch [23]. Lastly, double gas flows in this torch prevent reducing the shielding effect, which is a problem in the conventional GTAW process, as mentioned in [24-26].

5.2 Bead shape formation

In the case of the PAW process, the bead width on the bottom surface was close to the top surface. The plasma gas flow and the gas flow rate are very high. The arc is very constricted. It increases the risk of burn-through and blows away the metal in the molten pool in the case of very thin sheets. Meanwhile, in the case of GTAW welding, the bead width on

the top is much broader than the bottom surface due to low gas pressure. This is difficult to guarantee the strength of welded joints in stamping lines because the welded joints are cut, punched, bent, and pushed simultaneously. To solve both issues mentioned and obtain a more suitable welding process for ultra-thin sheets, a bead shape with a narrower on the top surface than GTAW but broader on the bottom surface than PAW will be a better solution. It is meaningful for this novel welding process.

Compared to the GTAW bead shape, the bead width on the top surface in the case of the novel GTAW is narrower, but the bead width on the bottom surface is wider. However, compared to the PAW process, the bead width in the case of the novel GTAW process is broader, especially on the top surface. As reported in [27], the bead width on the top and bottom surfaces in the PAW process was about 7.7 mm and 6.4 mm, respectively. Therefore, the ratio of bead width between the bottom and top surface was lowest in GTAW and highest in the case of PAW. Meanwhile, this ratio is located in the middle level for the case of the novel GTAW. This indicates that the novel technology features advantageous characteristics from GTAW and PAW processes. In other words, the bead width on the top surface is wider than the PAW process but narrower than the GTAW process, while the bead width on the bottom surface is broader than the GTAW process and narrower than the PAW process, as depicted in Figure 10.

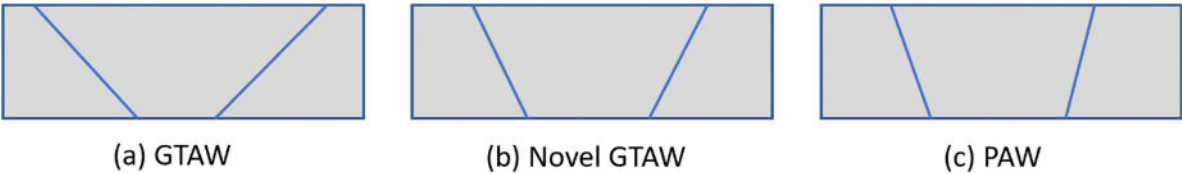


Figure 10. The schematic of bead shape in (a) GTAW process, (b) novel GTAW process, and (c) PAW process.

On the other hand, as shown in Figures 5 and 6, there are no welding defects such as convex, concave, and undercut at the weldment zone in the case of the novel torch. This is evidence that the constricted gas does not push down the molten metal to cause the dropping of the molten metal during the welding, even though the gas flows with high pressure and

speed. The reason is that, in novel technology, a low flow rate of input shielding gas and constricted gas is applied, 3.0 - 5.0 L/min for shielding gas and 1.5 - 2.0 L/min for constricting gas (Table 1). It means that it is “just enough” gas flow rate to maintain a stable arc plasma and will not cause defects. Meanwhile, the shielding gas flow rate is about 15 to 20 L/min in the GTAW process [28] and 10 to 15 L/min in the PAW process [29]. Hence, the production costs can be reduced by saving the shielding gas with the novel GTAW process.

Lastly, for the first time, an ultra-thin stainless steel sheet of 0.25 mm and 0.03 mm in thickness was butt welded completely by the novel GTAW process with high quality and no welding defects (Figures 5 and 6). The weldment height is similar to base metal thickness because no wire feeder was utilized. The bead is very stable, and its width is similar to the bead width in the laser welding process [13]. This is evidence that the novel GTAW process is ideal for replacing laser or electron beam welding processes that require very high investment costs.

5.3. Tungsten electrode lifetime and temperature

Another advantage of this novel orifice is that it increases the cooling rate for the tungsten electrode, thus decreasing the tungsten electrode temperature. This can be seen in Figure 7. The tungsten electrode is darker in the case of a novel GTAW process. Therefore, its life cycle is extended, leading to the corrosion of the tungsten electrode is significantly reduced, as shown in Figure 9. As a result, the stabilization of arc plasma is maintained for a long time. As seen in Figure 8 and the simulation results reported in [22], the tungsten electrode temperature distribution was much difference between the novel torch and the conventional torch. The temperature at the tip was much higher in the case of a conventional GTAW torch.

Moreover, the metal evaporation from the molten pool is essential for considering the superiority and difference between the novel GTAW and the conventional GTAW process. A fundamental difference between the novel GTAW torch and the conventional GTAW torch has been reported [22]. In the case of the conventional GTAW torch, the metal evaporation is much from the molten pool. They turn back and attach the tungsten electrode surface and the welded zone. Meanwhile, a low percentage of metal from the weld pool is favored in the case of the novel GTAW torch. It does not come back to the tungsten electrode and the welded zone as in the case of the conventional GTAW torch. The metal vapor is pushed

outside rather than returned to the tungsten electrode surface. The high-speed inner gas flow also cools the weld pool to decrease the evaporation and pushes the metal evaporation from the weld pool outside zones, as reported in [22]. This also prevents the attachment of evaporated metal on the tungsten electrode's tip and comes back to the weld pool to cause welding defects. As observed in Figure 9, the tungsten electrode is much cleaner in the novel GTAW torch than in the case of the conventional GTAW process.

5.4. Control the arc length

Typically, the arc length in the conventional GTAW process is challenging to set up at less than one millimeter. This is because the metal evaporation from the weld pool encloses the tungsten electrode tip to make a short-circuit, and molten pool surface fluctuation is too large [30, 31]. However, in the novel technology, the arc length can be set up at extremely short distances by reducing the evaporation from the molten pool and the contamination of the tungsten electrode surface. This was verified in this investigation (0.05 mm in the arc length for the 0.03-mm-thick sheets) and recent works, in which the arc length was set at 0.1 mm in the case of joining 0.1-mm-thick stainless steel SUS304 plates [32, 33]. This feature highlights the characteristics of the novel GTAW technology that it cannot establish in conventional GTAW processes. Relying on this advantage, the novel torch prevents the expansion of the arc plasma column (Figures 7 and 8).

In this novel system, a feedback control program is also developed with a circuit board to control the extreme shortness of the arc length. The servo motor moves the tungsten electrode from the original point above the base metal. When the tungsten electrode tip is contacted with the base metal, the signal is feedbacked to the circuit board through a control program to divert the rotation of the motor. An original point has been set up before; thus, the program will automatically calculate the distance between the base metal and the tungsten electrode tip to detect the arc length correctly. This control technology is essential and valuable for joining ultra-thin sheets in the extreme shortness of the arc length.

5.5. The balance of heat input in the molten pool

Usually, controlling heat input is considered the principal matter in welding thin and ultra-thin sheets. The issue for welding ultra-thin sheets depends not only on the control of heat input but also on the balance of the heat input supplied to the weld pool. Herein, such a balance is the heat input distribution at both sides of the weld pool (left and right). It opposes the torch is shifted to the left or right side of the butt joint line. In that case, the highest

temperature location of the arc plasma column is also shifted, resulting in the burn-through phenomenon of the workpiece in the shifted direction. However, the partner site and the butt joint position are insufficient to melt by heat input. Therefore, it is difficult to form a sound welded joint. Furthermore, using the long novel orifice along the tungsten electrode inside the novel torch prevents the change of the relative position between the tungsten electrode and the welded location. In this case, the balance of heat input is maintained well. The novel orifice guides the position of the electrode tip and maintains that location unchanged in every case, even if the electrode is moved out to repair its tip shape and reinstall it into the torch. Such benefits are generally challenging to be achieved in conventional GTAW or PAW processes.

In summary, the novel GTAW process can be accomplished superiority points of both GTAW process and PAW processes, such as low heat input, high heat input density, constricted arc, low metal evaporation, low-temperature tungsten electrode, reduced burn electrode tip, arc stability, and reliability in thin/ultra-thin welding sheets. As a result, a high-speed welding and reliable butt weld with free defects for thin/ultra-thin metal sheets can be obtained. In other words, the novel torch simultaneously commanded the heat input with very high accuracy. This novel technology is the potential to compete with advanced welding processes such as laser and electron beam welding for ultra-thin metal sheets. The developed novel technique is an ideal and promising solution for improving the quality and productivity in manufacturing high-precision and high-tech products of ultra-thin sheets in automatic production lines. The application of this novel solution increases productivity and efficiency and creates sustainable production and a green manufacturing environment.

6. Conclusions

In this study, a novel GTAW process for butt-joint of material coils in production lines has been presented and discussed. By developing a novel welding torch with superior characteristics compared to the conventional GTAW and PAW, the novel technique becomes an ideal solution for joining thin and ultra-thin metal sheets. Some key insights can be drawn as follows:

- The novel GTAW process is better than the conventional GTAW process by combining advantageous characteristics of both GTAW and PAW processes.

- The weld profile produced by the novel GTAW process is wider on the bottom surface but narrower on the top surface than the conventional GTAW process.
- The shielding constricted gas efficiently cools the tungsten electrode and minimizes the burning phenomena at the electrode tip.
- The heat input is decreased, but its density is increased at the center area.
- The tungsten electrode position can be fixed (no oscillation) to improve the heat input balance at each welding position.
- The novel GTAW process enables butt welding of thin and ultra-thin metal sheets (up to 0.03 mm) with high accuracy and reliability.

Funding: This research is supported by Vingroup Innovation Foundation (VINIF) in project code VINIF.2020.DA12

Conflicts of Interest: The authors declare that there is no conflict of interest regarding the publication of this paper.

References

- [1] Takeda Y, Hayasaka K, Shiwaku R, Yokosawa K, Shiba T, Mamada M, et al. Fabrication of Ultra-Thin Printed Organic TFT CMOS Logic Circuits Optimized for Low-Voltage Wearable Sensor Applications. *Scientific Reports* 2016;6:25714. <https://doi.org/10.1038/srep25714>.
- [2] Tisza M, Czinege I. Comparative study of the application of steels and aluminum in lightweight production of automotive parts. *International Journal of Lightweight Materials and Manufacture* 2018;1:229–38. <https://doi.org/10.1016/j.ijlmm.2018.09.001>.
- [3] TE_Connectivity. Connectors for Aerospace, Defense and Marine n.d. https://www.peigenesis.com/images/content/pei_tabs/te-connectivity/te_connectivity-1052982-1-datasheet.pdf (accessed April 5, 2022).
- [4] ABLOY TE, ZUHAILAWATI H, AIZAD S, ANASYIDA AS. Geometrical, microstructural and mechanical characterization of pulse laser-welded thin sheet 5052-H32 aluminum alloy for aerospace applications. *Transactions of Nonferrous Metals Society of China* 2019;29:667–79. [https://doi.org/10.1016/S1003-6326\(19\)64977-0](https://doi.org/10.1016/S1003-6326(19)64977-0).
- [5] Cheng Z, Li Y, Xu C, Liu Y, Ghafoor S, Li F. Incremental sheet forming towards biomedical implants: a review. *Journal of Materials Research and Technology* 2020;9:7225–51. <https://doi.org/10.1016/j.jmrt.2020.04.096>.
- [6] Badgujar TY, Wani VP. Performance Study of Stamping Process Using Condition Monitoring: A Review. *Lecture Notes in Mechanical Engineering*, Springer Singapore; 2019, p. 521–9. https://doi.org/10.1007/978-981-13-2490-1_48.
- [7] TE_Connectivity. TE Connectivity Named One of China’s 50 Most Innovative Companies of 2016 By Fast Company China n.d.
- [8] Singh J, Laurenti R, Sinha R, Frostell B. Progress and challenges to the global waste

- management system. *Waste Management & Research: The Journal for a Sustainable Circular Economy* 2014;32:800–12. <https://doi.org/10.1177/0734242X14537868>.
- [9] Chaudhary J, Jain NK, Pathak S, Koria SC. Investigations on thin SS sheets joining by pulsed micro-plasma transferred arc process. *Journal of Micromanufacturing* 2019;2:15–24. <https://doi.org/10.1177/2516598418820470>.
- [10] Tseng KH, Hsieh ST, Tseng CC. Effect of process parameters of micro-plasma arc welding on morphology and quality in stainless steel edge joint welds. *Science and Technology of Welding and Joining* 2003;8:423–30. <https://doi.org/10.1179/136217103225009107>.
- [11] Hong Y, Chang B, Peng G, Yuan Z, Hou X, Xue B, et al. In-process monitoring of lack of fusion in ultra-thin sheets edge welding using machine vision. *Sensors (Switzerland)* 2018;18. <https://doi.org/10.3390/s18072411>.
- [12] Long H, Gery D, Carlier A, Maropoulos PG. Prediction of welding distortion in butt joint of thin plates. *Materials & Design* 2009;30:4126–35. <https://doi.org/10.1016/j.matdes.2009.05.004>.
- [13] Ismail MIS. *Micro-welding of Engineering Materials by High Brightness Lasers*. Ph.D. thesis OKAYAMA UNIVERSITY, 2012.
- [14] Hailat MM, Mian A, Chaudhury ZA, Newaz G, Patwa R, Herfurth HJ. Laser micro-welding of aluminum and copper with and without tin foil alloy. *Microsystem Technologies* 2012;18:103–12. <https://doi.org/10.1007/s00542-011-1378-8>.
- [15] Verma M, Ahmed S, Saha P. Challenges, process requisites/inputs, mechanics and weld performance of dissimilar micro-friction stir welding (dissimilar μ FSW): A comprehensive review. *Journal of Manufacturing Processes* 2021;68:249–76. <https://doi.org/10.1016/j.jmapro.2021.05.045>.
- [16] Scialpi A, De Giorgi M, De Filippis LAC, Nobile R, Panella FW. Mechanical analysis of ultra-thin friction stir welding joined sheets with dissimilar and similar

- materials. *Materials & Design* 2008;29:928–36.
<https://doi.org/10.1016/j.matdes.2007.04.006>.
- [17] Huang Y, Meng X, Zhang Y, Cao J, Feng J. Micro friction stir welding of ultra-thin Al-6061 sheets. *Journal of Materials Processing Technology* 2017;250:313–9.
<https://doi.org/10.1016/j.jmatprotec.2017.07.031>.
- [18] Yamamoto H, Aoyama Y, Ito K, Yamada T, Tanaka M, Hoshikawa H, et al. Friction stir welding of ultra-high-purity aluminum thin sheets never to lower high conductivity at ultra-low temperature. *Welding International* 2020;34:125–37.
<https://doi.org/10.1080/09507116.2021.1921983>.
- [19] Mao Y, Ni Y, Xiao X, Qin D, Fu L. Microstructural characterization and mechanical properties of micro friction stir welded dissimilar Al/Cu ultra-thin sheets. *Journal of Manufacturing Processes* 2020;60:356–65.
<https://doi.org/10.1016/j.jmapro.2020.10.064>.
- [20] Meghan H, Dehghani K, Shafiei A. Effects of process parameters on microstructure and mechanical properties of Al_{0.5}CoCrFeNi high entropy alloy thin sheets using pinless friction stir welding. *Journal of Materials Research and Technology* 2022;16:1069–89. <https://doi.org/10.1016/j.jmrt.2021.12.050>.
- [21] Lee SS, Kim TH, Hu SJ, Cai WW, Abell JA. Joining technologies for automotive Li-ion battery manufacturing – A REVIEW. *Proceedings of the ASME 2010 International Manufacturing Science and Engineering Conference (MSEC2010)*, 2010, p. 1–9.
- [22] Nguyen VA, Seongming H, Nguyen HM, Murata A, Tinh D, Quy L, et al. A novel welding solution of intelligent production system for heat exchanger equipment and lithium battery in the electric vehicle. *Sheet Metal Welding Conference XIX: Welding Solutions for Lightweight and Electric Vehicle Production*, American Welding Society, Livonia USA: 2021.

- [23] Tanaka Manabu, Tashiro Shinichi. A Study of Thermal Pinch Effect of Welding Arcs. *QUARTERLY JOURNAL OF THE JAPAN WELDING SOCIETY* 2007;25:336–42. <https://doi.org/10.2207/qjws.25.336>.
- [24] Li D, Lu S, Li D, Li Y. Effect of Structural Parameters of Double Shielded TIG Torch on the Fusion Zone Profile for 0Cr13Ni5Mo Martensitic Stainless Steel. *Journal of Materials Science & Technology* 2014;30:922–7. <https://doi.org/10.1016/j.jmst.2013.12.012>.
- [25] Lu Shanping, Li Dongjie, Li Dianzhong, Li Yiyi. Double shielded TIG welding method. *Transactions of the China Welding Institution* 2010; 31(2): 21-24.
- [26] LI Dongjie, LU Shanping, LI Dianzhong, LI Yiyi. Tracer investigation of convection in weld pool under TIG welding process. *Transactions of the China Welding Institution* 2011; 32(8): 45-48.
- [27] Van Nguyen A, Tashiro S, Ngo MH, Van Bui H, Tanaka M. Effect of the eddies formed inside a weld pool on welding defects during plasma keyhole arc welding. *Journal of Manufacturing Processes* 2020;59:649–57. <https://doi.org/10.1016/j.jmapro.2020.10.020>.
- [28] Liu YK, Zhang WJ, Zhang YM. A tutorial on learning human welder's behavior: Sensing, modeling, and control. *Journal of Manufacturing Processes* 2014;16:123–36. <https://doi.org/10.1016/j.jmapro.2013.09.004>.
- [29] Van Nguyen A, Tashiro S, Ngo MH, Le AH, Van Bui H, Tanaka M. Influence of shielding gas composition on molten metal flow behavior during plasma keyhole arc welding process. *Journal of Manufacturing Processes* 2020;53:431–7. <https://doi.org/10.1016/j.jmapro.2020.03.031>.
- [30] Dai H, Shen X, Wang H. Study on the arc pressure of TIG welding under the condition of Ar-Ar and Ar-He supply alternately. *Results in Physics* 2018;10:917–22. <https://doi.org/10.1016/j.rinp.2018.08.015>.

- [31] Wang X, Huang J, Huang Y, Fan D, Guo Y. Investigation of heat transfer and fluid flow in activating TIG welding by numerical modeling. *Applied Thermal Engineering* 2017;113:27–35. <https://doi.org/10.1016/j.applthermaleng.2016.11.008>.
- [32] Nguyen VA, Huu MN, Akihisa M, Tashiro S, Tanaka M. Research and Development of Comprehensive Solution for Joining Ultra-thin Sheet Using in Smart Production Lines. *AWS Education 2020 Virtual Summit, Las Vegas-USA*: 2021.
- [33] Anh N Van, Akihisa M, Tadasuke M, Tashiro S, Tanaka M. Influence of Welding Current on Formation of Weld Bead in TIG Welding for Joining Thin Plates. *Advanced Engineering Forum* 2018;29:1–11. <https://doi.org/10.4028/www.scientific.net/AEF.29.1>.

Development of a novel GTAW process for joining ultra-thin metal sheets

Manh, Ngo Huu

2022-06-23

Attribution-NonCommercial-NoDerivatives 4.0 International

Manh NH, Nguyen VA, Duy HL, et al., (2022) Development of a novel GTAW process for joining ultra-thin metal sheets. *Journal of Manufacturing Processes*, Volume 80, August 2022, pp. 683-691

<https://doi.org/10.1016/j.jmapro.2022.06.043>

Downloaded from CERES Research Repository, Cranfield University